IMPORTANCE OF CRACK OPENING IN UT INSPECTION QUALIFICATION

Mika Kemppainen, Iikka Virkkunen, Trueflaw Ltd., Finland
Tapani Packalén, Juha Sillanpää, Inspecta Certification Oy, Finland
Raimo Paussu, Fortum Nuclear Services Oy, Finland

ABSTRACT

Good, representative cracks are needed for reliable qualification. The qualification cracks should be representative of the expected in-service cracks in terms of essential characteristics that affect the inspection in question. For UT inspection, one such important characteristic is the crack opening.

In order to find out the importance of crack opening to UT inspection qualification and to quantify and compare the available artificial flaw production technologies, a research project "Avauma" was carried out. The project included participants from the Finnish qualification body (Inspecta Certification), the Finnish utilities (TVO and Fortum), the Finnish NDT vendors (Polartest, VTT, Inspecta), and the Finnish flaw producers (Trueflaw, Fortum Nuclear Services). In the project, significance of crack opening on different ultrasonic techniques and inspection procedures is quantified, and conclusions drawn for further development of Finnish qualification practice.

Cracks used in the project were produced by state of the art crack producing techniques capable of producing controlled, realistic cracks with known size and opening. Applied crack producing techniques are widely used in Finnish qualification processes, and similar techniques are considered for the qualification processes used for new plants, as well.

22 cracks in total were produced with different crack openings using three different crack production techniques. For some of the cracks, the opening was modified after the production with thermal loading to obtain wider range of crack openings. The samples were inspected by different ultrasonic techniques, procedures and by various inspectors. Finally, the samples were destructively studied to reveal the metallographic characteristics of the flaws. The flaw opening along the crack depth and other flaw characteristics were measured from the metallographic samples.

In the present paper, the metallographic crack properties are documented and discussed. The paper presents the quantitative metallographic results together with selected NDE results. Results of the destructive testing are compared to the reported NDE results. The significance of the crack opening to the performance of different ultrasonic techniques and various inspection procedures is assessed. Metallographic results are also compared to the corresponding results from service-induced cracks, as reported in the open literature.

The capabilities of different crack manufacturing techniques are analysed and discussed in terms of crack opening and its controllability, resulting crack characteristics, and the overall ability to achieve realistic artificial cracks with variable crack opening.

INTRODUCTION

Representative cracks are needed for reliable qualification. The qualification cracks should be representative of the expected in-service cracks in terms of essential characteristics affecting the inspection in question. Also, the artificial cracks should not contain any such features, that are not present in the expected in-service cracks and that would affect the performance or reliability of the inspection [1].

The previous studies on different flaw manufacturing techniques (refs. 2 and 3) underline the need for better understanding of the effects of non-similarities between artificially produced reflectors and service-induced cracks to NDE response in qualification. Furthermore, those studies expressed need for having better flaw manufacturing techniques not exhibiting weaknesses shown, e.g., in the flaws used during the first ENIQ pilot study [2]. After these studies, a new technology has been developed to meet this requirement [4].

For UT inspection, one important characteristic is expected to be the crack opening. Crack opening, in general, affects the UT response obtained from the crack. Greater opening is associated with stronger signal. It has been reported, that with very small opening, the crack may become at least partly transparent to ultrasound [5]. The crack tip signal, in particular, is sensitive to crack tip opening. Crack tip signal is crucial in many sizing techniques and hence it is important to faithfully reproduce the crack tip signal for sizing qualification. Though there have been several studies on the effect of crack mouth opening to NDE response (e.g., references 5, 6, and 7), much less studied is the effect of the opening distribution of the whole crack, and opening at the crack tip, to the NDE response. It is also essential to compare such studies to information published about the opening of real, service-induced flaws to have a connection to the qualification and its targets.

Typical crack opening values in service

Natural service-induced cracks exhibit a wide variety of different openings. This results from the wide variety of different loading conditions and mechanisms effective in operational conditions inducing cracks, as well as the material properties of the material in question.

Wåle [8] has measured crack mouth and tip openings from numerous service-induced cracks. These values are summarized in Figures 1 and 2, respectively. It should be noted that bigger cracks with wider opening are more likely to be found. Consequently, the data is likely to be biased and the population shows too great opening values. Furthermore, these measurements were done from images in existing failure analyses. The primary objective of such analyses has been other than crack characterization for NDE and, consequently, all crack characteristics may not be readily observable from the images present. In particular, the crack tip radius is generally not well described in failure analyses.

Crack opening values for different artificial flaw manufacturing techniques have been measured from images present in the open literature [9] by Virkkunen et al. [11]. These measurements represent values from numerous flaw manufacturers using crack simulation techniques and solidification cracks. This data is also summarized in Figures 1 and 2. When reading the data, it should be noted, that measurement of crack opening values from the images was rather difficult and, hence, the accuracy of the numbers is limited.

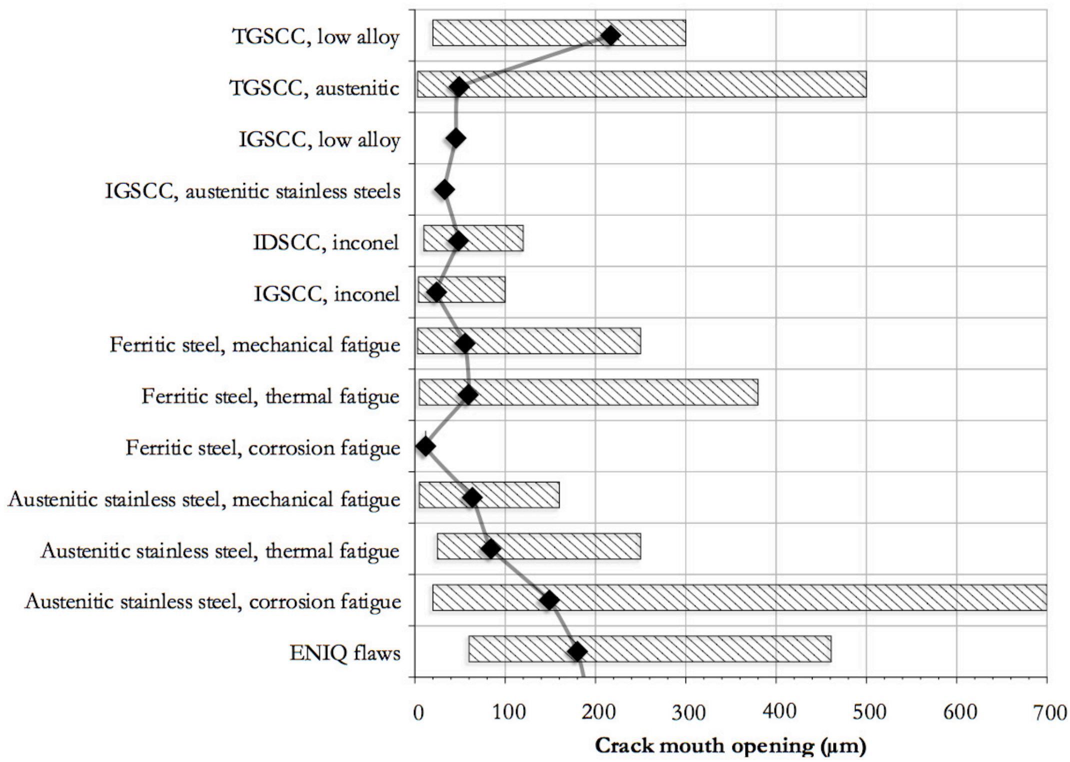

Figure 1 **Crack mouth opening (CMO) values of service-induced cracks and artificial cracks, in µm. The bars show the range between minimum and maximum values reported. The dots connected by line show the average value reported. Note, that the average value tends to be closer to minimum than maximum. Values for service-induced flaws were taken from [8]. Values for artificial flaws were measured from [9].**

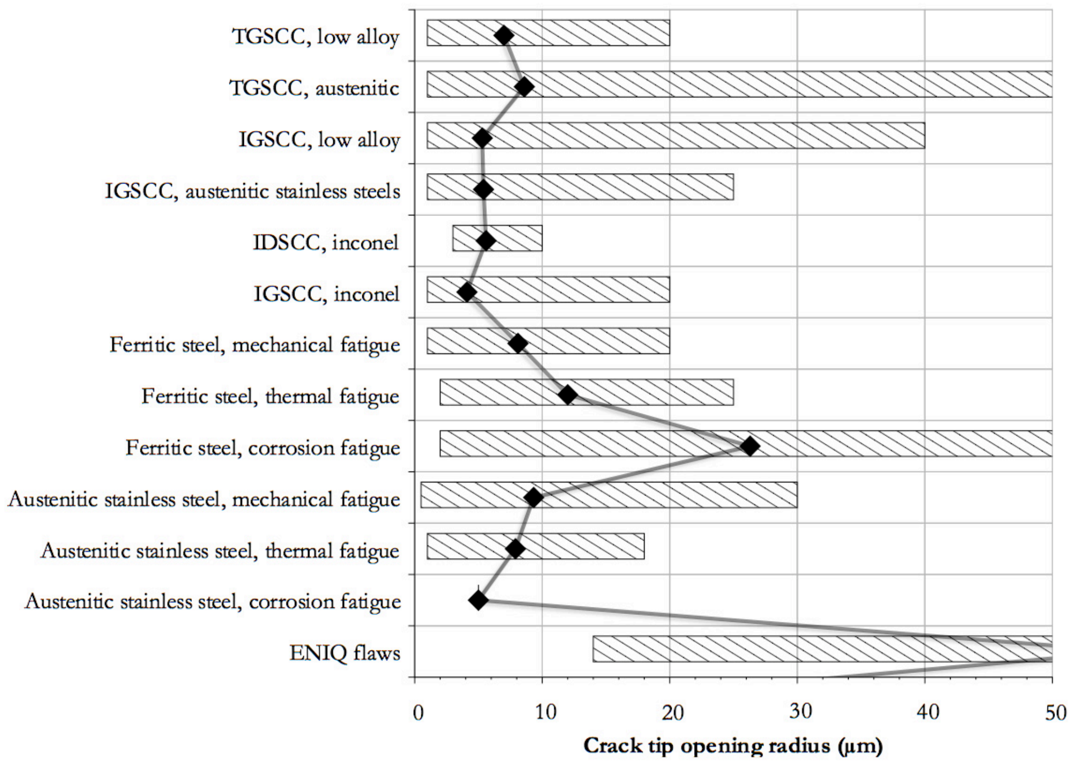

Figure 2 **Crack tip opening radius (CTO) values of service-induced cracks and artificial cracks, in µm. The bars show the range between minimum and maximum values reported. The dots connected by line show the average value reported. Note, that the average value tends to be closer to minimum than maximum. Values for service-induced flaws were taken from [8]. Values for artificial flaws were measured from [9].**

AIM OF PRESENT WORK

The aim of present work was to compare available artificial flaw production technologies, produce solid metallographic data on the characteristics of different artificial flaws and to find out the importance of crack opening to UT inspection qualification.

MATERIALS AND METHODS

Three different flaw manufacturing techniques were used in this work for flaw production, two of them included welding. The aim was to produce artificial flaws with different techniques commonly used in today's qualification samples. The produced samples were inspected by popular inspection methods currently used in Finland. Finally, the samples were destructively examined and relevant crack characteristics measured.

The results of the performed study are reported in three publications. The current work reports the metallographic results. Packalén et al. [10] analyse the NDE results. Paussu et al. [12] discuss the project from the utility perspective.

Flaw production techniques

Three flaw manufacturing techniques were used in this study. Two of these are welding-based: "solidification cracks" and "weld joined fatigue surfaces". Third technique "thermal fatigue crack" does not include welding.

Solidification cracks are produced as follows: an excavation is ground in the place, where crack is to be introduced. The excavation is filled by welding with suitable filler material and welding parameters to create a solidification crack in the middle of each weld pass. Finally, the surface of the weld is ground to the final shape. The final depth is controlled by the depth of the opening ground on the surface, and control of the solidification process. The target depth is the depth of the opening. However, there is variance in the cracking of the first weld pass when filling the opening. Variance in the solidification process and possible machining give rise to the characteristic depth tolerance for the process. The tolerance given by the manufacturer is ±1.0 mm.

The flaw type "weld joined fatigue surfaces" is produced in three steps with an assistance of an aid piece. First the aid piece is welded on the side wall of the prepared weld groove, and manually loaded to create a fatigue crack. The loading is continued until separation. The created fatigue surfaces of the aid piece are then manually ground to the desired shape. Shaped fatigue surfaces are welded tightly together and back to side wall, and welding of the actual joint is completed. Finally, the surface of the weld is ground to the final shape. The final depth is determined by the size of the shaped surfaces and the fixing welding procedure. The target depth is the depth of the shaped fatigue surface subtracted by the weld pass penetration of the fixing weld and machining thickness. Depth tolerance of this flaw type comes from the variations of the penetration of the joint weld pass in the edge of the fatigue surfaces and machining. The tolerance given by the manufacturer is ±1.0 mm.

Flaw production by thermal fatigue is done in-situ with ready-made sample. The cyclic thermal fatigue loading is induced locally by alternating heating and water spray cooling, as described by Kemppainen [4]. The loading is based on pure thermal loading and there is no welding, machining, or any other mechanical treatment applied. The final depth is based on the applied process parameters (strength of the loading cycle, and amount of applied total cycles). Appropriate parameters are verified in advance by destructive validation, i.e. a crack is produced to similar material and destructively tested to reveal its true size. The best estimate depth is the statistical average depth from several validations. The tolerance comes from the statistical variance of validation results. The tolerance given by the manufacturer is ±1.0 mm. The opening of thermal fatigue cracks is based on variation of the applied process loading parameters. In this work, cracks with different openings were produced by applying different combinations of post-production loading sequences. The opening manipulation was done for six flaws with qualitative aim of seeing the effect of different combinations of loading parameters.

Specimens and materials

Solidification cracks and weld joined fatigue surfaces were produced to an austenitic stainless steel plate specimen with a X-groove butt-weld in the middle of the plate. Plate dimensions were 400 mm x 300 mm x 30 mm (length x width x thickness). In addition, two solidification cracks were produced to a ferritic base metal plate with dimensions of 400 mm x 300 mm x 30 mm (length x width x thickness).

Thermal fatigue cracks were produced to two ready-made austenitic stainless steel base material plates with dimensions of 300 mm x 300 mm x 20 mm (length x width x thickness). Four cracks were produced to each plate, the other plate having cracks with 3 mm and the other one with 6 mm target depths. Cracks were produced in the centreline of the specimens.

Destructive examination

The produced flaws were destructively examined to reveal their characteristics. The measurements were conducted from high-resolution digital images using semi-automatic image analysis software "CrackMeasure" written by Trueflaw. The characteristics measured were similar to those measured by Wåle [8]. However, with automated measurement program and with metallographic samples made for this purpose in particular, much more detailed and accurate results were obtained. The measurements were done for the surface of the sample and for cross-section.

Metallographic sample was prepared for each crack. The samples were manufactured with special care taken to ensure that crack opening was not altered in sample production. The cross-sectional sample was taken close to the deepest location of the flawed samples. Cross-sections were polished with normal metallographic procedure, and etched with appropriate etchant. Both the as-polished and etched surfaces were measured, because etching of the cracked area always rounds the corners of the fracture surface making the opening look bigger in the micrographs.

Finally the cross-sectional samples were bent open to reveal the true depth and shape of the flaws and the opened surface was photographed. The destructive analysis was supervised by Inspecta Certification in order to ensure impartial and objective measurements.

RESULTS

Metallographic data

The measured opening values as well as target and destructively revealed true depths for all the produced cracks are tabulated in Annex 1. Furthermore, the best estimate values as given by the manufacturer, are given for the thermal fatigue cracks. For opening, four values are reported: near mouth opening, middle opening, near tip opening and tip opening. The three first are reported as average measured opening from 0.5 mm length. Tip radius measurement was done by fitting a circle to high-magnification image of the crack tip and measuring its radius.

The specified tolerance for all flaw types for length and depth were ±2 mm and ±1 mm, respectively. The actual correspondence between the specified, best estimate, and true depth values for the thermal fatigue cracks is presented in Figure 3.

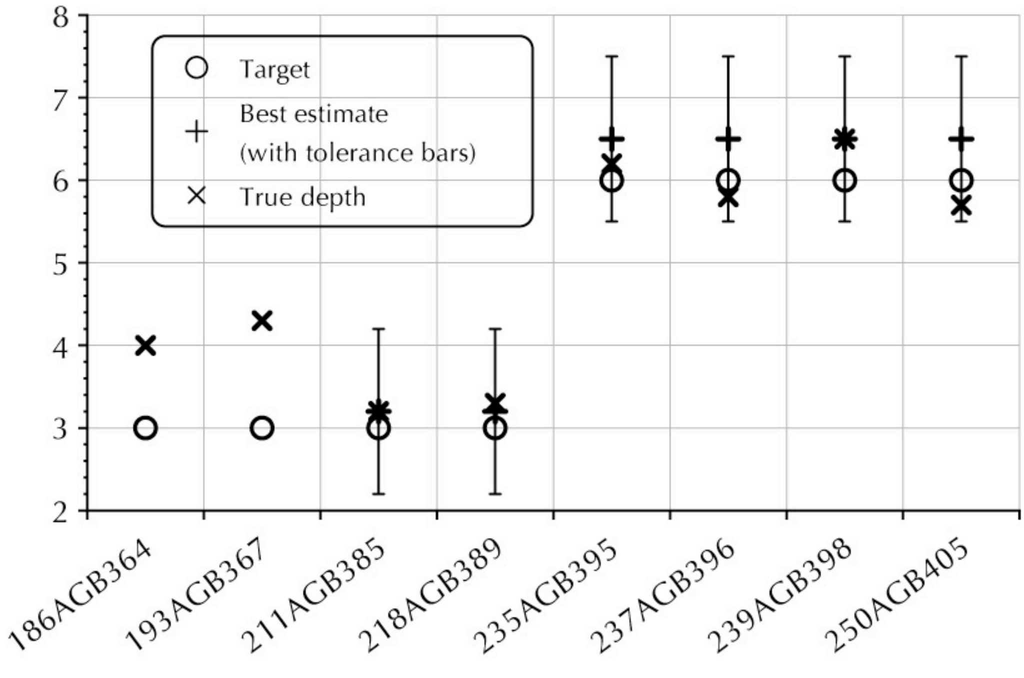

Figure 3 Comparison of specified, best estimate and true depth of the flaws, together with tolerance range given by the manufacturer.

Opening manipulation of thermal fatigue cracks

Post-production manipulation of the opening was performed for six thermal fatigue cracks. Different loadings were used to get different changes in the crack openings and the result of opening manipulation was measured on the surface opening. Surface opening values for all the produced thermal fatigue cracks are tabulated in Table 1. A graphical example of the comparison between the surface opening profiles for the as-produced and as-manipulated conditions of one crack is shown in Figure 4.

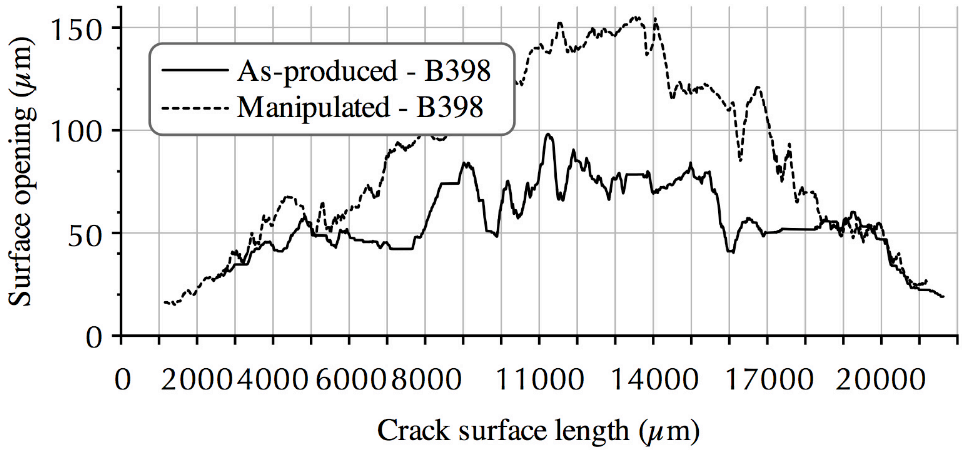

Figure 4 Surface opening of a thermal fatigue crack (239AGB398) in as-produced condition and after opening manipulation.

Table 1 Values for surface openings for thermal fatigue cracks in as-produced and as-manipulated conditions.

Flaw ID	As-produced (μm)	Opening modified (μm)
186AGB364	60	78
193AGB367	67	92
211AGB385	70	-
218AGB389	46	65
235AGB395	123	127
237AGB396	51	-
239AGB398	82	139
250AGB405	130	103

Another aspect on the crack opening is the opening distribution in the depth direction of the crack. The difference in depth direction of an as produced and opening manipulated crack was revealed by comparing the measured cross-sectional openings of two different cracks, as the example shows in Figure 5. Both cracks were produced with the same process, the other one was left in as-produced condition while the other one was manipulated to have bigger opening.

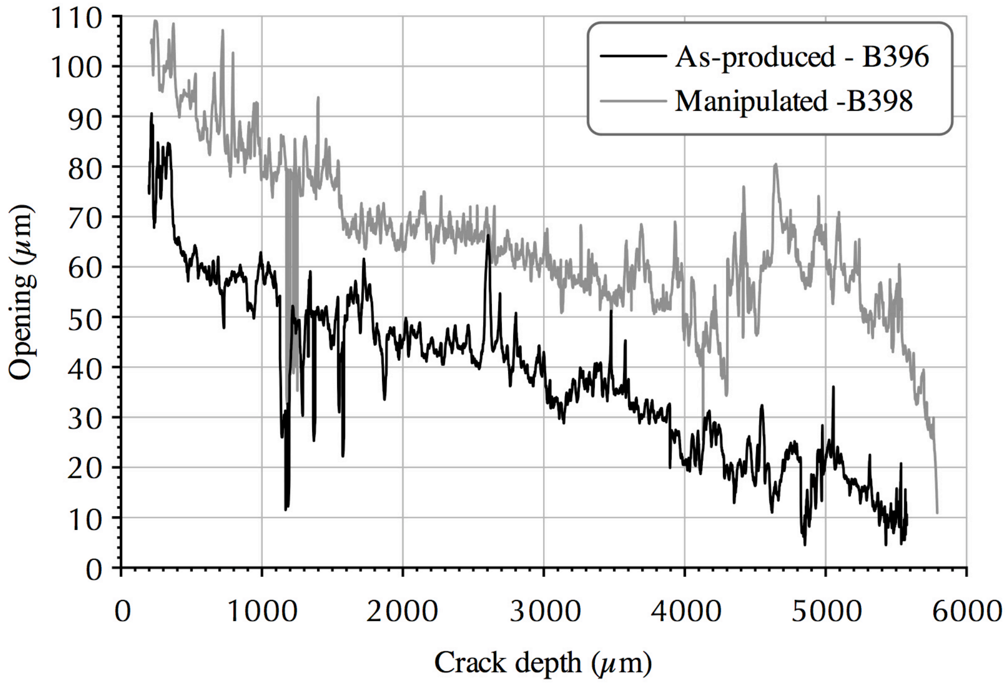

Figure 5 **Opening profiles in cross-section of two cracks in as-produced and manipulated conditions, (237AGB396 and 239AGB398, respectively).**

Metallographic characteristics of flaws

The metallographic images of the three different flaw types manufactured in the project reveal clear differences in their typical flaw appearances. Examples of cross-sectional images of solidification flaws, weld joined fatigue surfaces, and thermal fatigue cracks are shown in Figures 6, 7, 8 and 9, respectively. Two examples are shown for the weld joined fatigue surfaces. These images are selected to show certain features and they do not exhibit cross-sections typically produced by the welding-based techniques, as declared by the manufacturer.

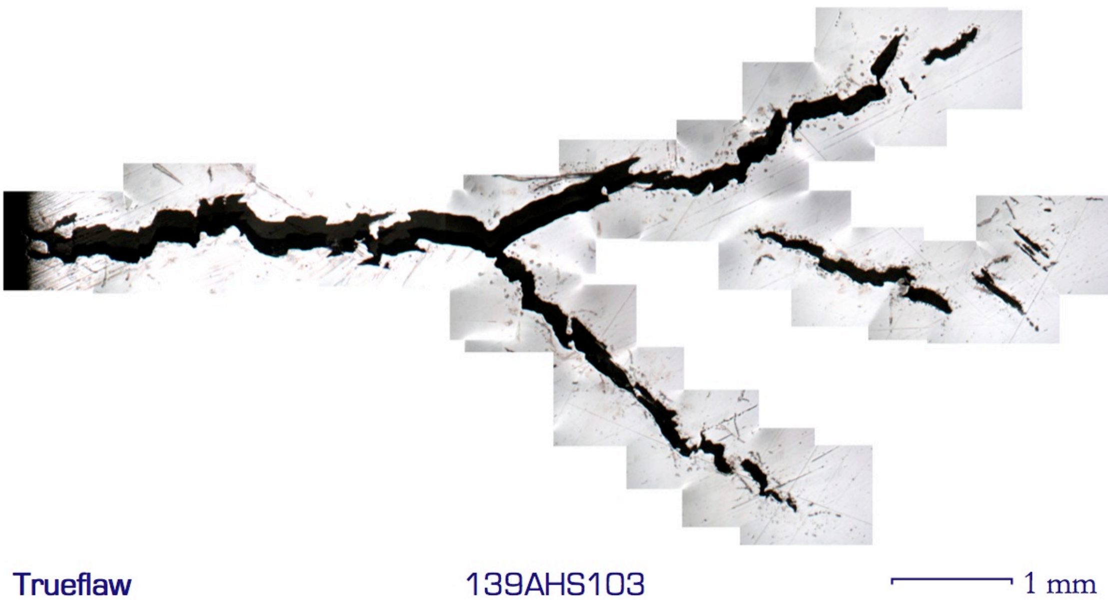

Figure 6 **Cross-sectional image of a solidification crack (flaw 139AHS103).**

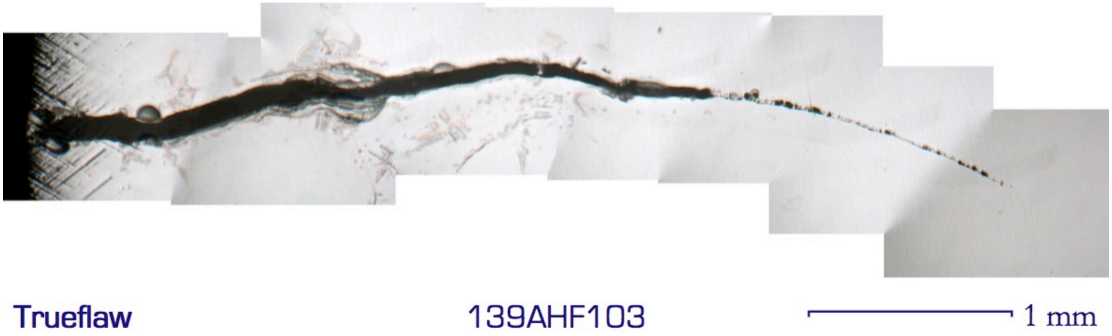

Figure 7 Cross-sectional image of a weld joined fatigue surface (flaw 139AHF103).

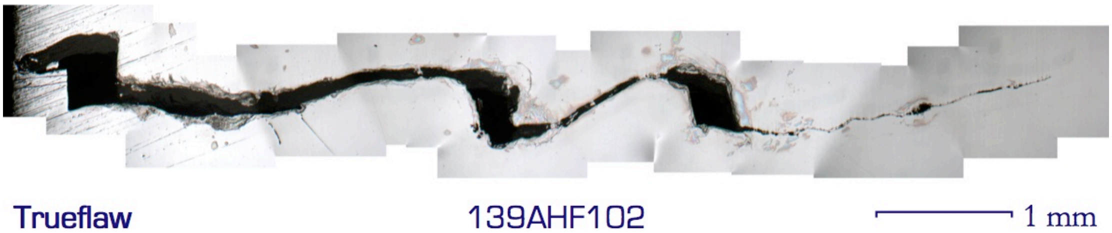

Figure 8 Cross-sectional image of a weld joined fatigue surface (flaw 139AHF102).

Figure 9 Typical cross-sectional image of a thermal fatigue crack with opening modified to larger value (crack 239AGB398).

DISCUSSION

Characteristic features of used flaw manufacturing techniques

Three flaw manufacturing techniques were used in this study. Two of these are welding-based: "solidification cracks" and "weld joined fatigue surfaces". Third technique "thermal fatigue crack" does not include welding. The flaws were produced by two companies, Fortum Nuclear Services (solidification cracks and weld joined fatigue surfaces) and Trueflaw (thermal fatigue cracks). Thermal fatigue crack production technique is exclusively used by Trueflaw. The other two techniques are widely used by other flaw manufacturers, besides Fortum Nuclear Services. Consequently, it is of interest to compare the flaws analyzed here with those produced by other manufacturers using the same technique. Lemaitre et al. [9] and more recently Iacono et al. [3] have reported cross-section images from flaws manufactured by numerous artificial flaw production companies. Comparison with these publications reveals, that the features reported in this study represent the typical features of the used manufacturing techniques in general, and the results are applicable for all flaws manufactured by the studied techniques.

In the cross-sectional images of the destructive testing results, it is seen that weld joined fatigue surfaces are located on one side of the joint weld and have weld metal on both sides resulting from the welding of the small aid piece to the wall of the original weld groove. Crack tips are melted by the welding and they exhibit relatively small radius. In the shallow surface layer these flaws have very small opening caused by the machining process.

Solidification flaws are located in the middle of the weld passes. These flaws have relatively large openings through their whole depth. Furthermore, solidification flaws produced in austenitic stainless steel have major branches and unbroken ligaments causing the special aspects in their NDE response. In the shallow surface layer the solidification flaws have very small opening caused by the machining process.

Thermal fatigue cracks are located in the base metal without introducing any other changes in the material. Especially, there is no welding done during the process. These cracks are tight, have natural propagation through the microstructure, and have small crack tip radiuses. The applied opening treatment of six of the cracks had changed their opening markedly. The opening profile in depth direction is natural exhibiting largest opening at the surface and smallest at the crack tip.

Deviation between the best estimate and true depth values from the destructive testing reveal that thermal fatigue cracking process is well in line with the by manufacturer given characteristic tolerances of the technique.

Comparison between different flaw types and service-induced cracks

One of the aims of this study was to compare the characteristics of artificial flaws made with different techniques with the actual, service induced flaws as described in the Wåle report [8]. Figure 9 and 10 show the literature data together with data produced in the "Avauma" project.

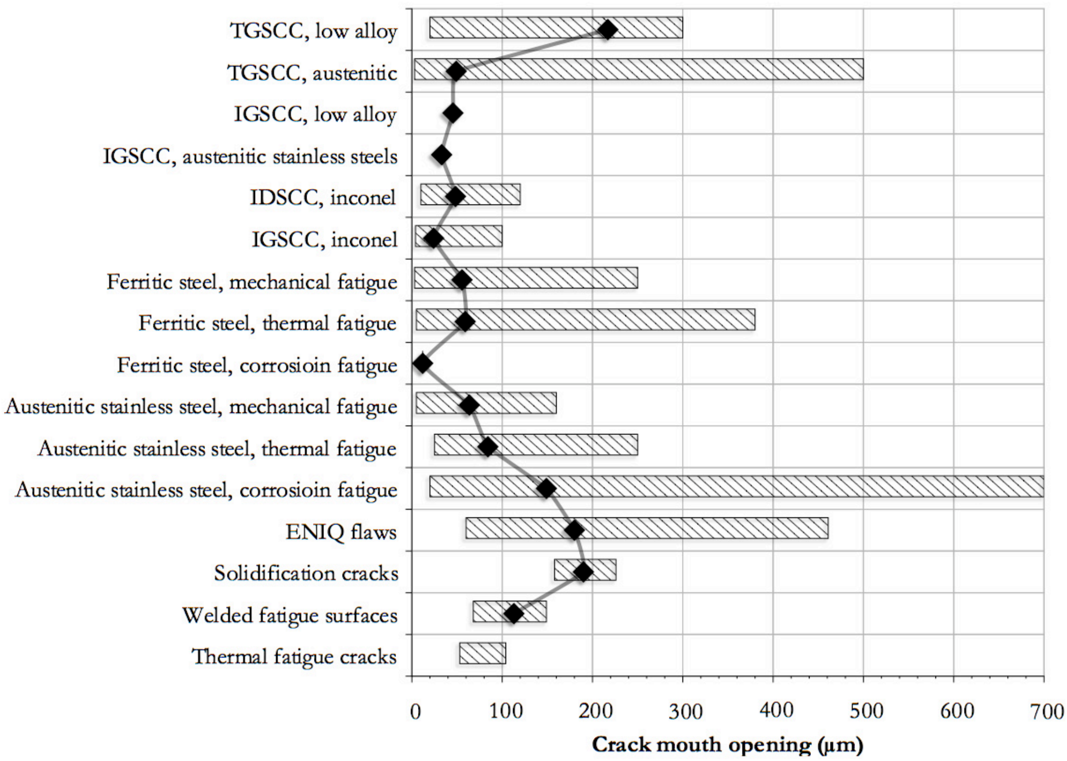

Figure 10 **Crack mouth opening (CMO) values of service-induced cracks and artificial cracks, in μm. The bars show the range between minimum and maximum values reported. The dots connected by line show the average value**

reported. Note, that the average value tends to be closer to minimum than maximum. For Thermal fatigue cracks, average values are not reported. For this flaw type, the opening can be produced to specified value within the range given. Values for service-induced flaws were taken from [8]. Values for "ENIQ" flaws were taken from [11].

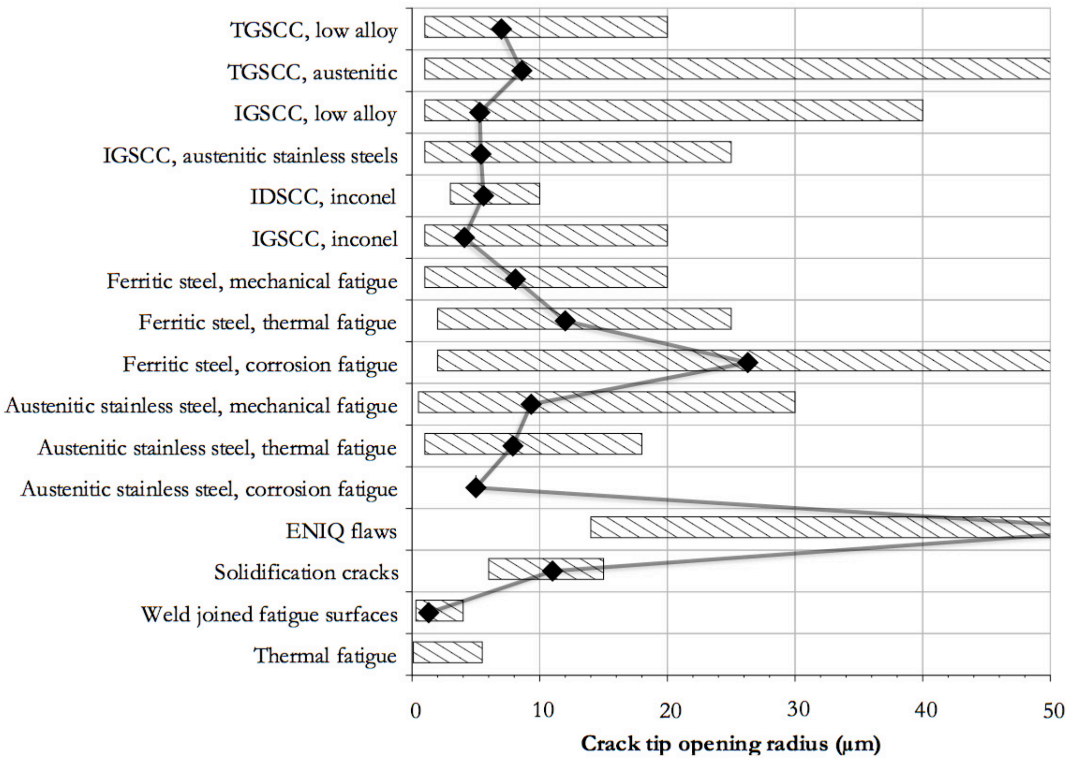

Figure 11 Crack tip opening radius (CTO) values of service-induced cracks and artificial cracks, in µm. The bars show the range between minimum and maximum values reported. The dots connected by line show the average value reported. Note, that the average value tends to be closer to minimum than maximum. For Thermal fatigue cracks, average values are not reported. For this flaw type, the opening can be produced to specified value within the range given. Values for service-induced flaws were taken from [8]. Values for "ENIQ" flaws were taken from [11]. Note also, that the crack-tip-radius values measured in this study were taken from polished (not etched) high-magnification images taken especially for this purpose. In contrast, the measurements from [8] and [11] are taken, in general, from etched lower magnification images. Consequently, the values taken from [8] and [11] may show greater values than would be correct.

The above figures show the correspondence of the different artificial flaws to real, service-induced cracks. In addition, different flaw manufacturing techniques are divided to "ENIQ" flaws and flaws produced in this study. In the Figure 10 the range and average values for the "ENIQ" flaws are bigger than values for the most of the service-induced cracks. "ENIQ" flaws included both solidification flaws and weld joined fatigue surfaces.

Solidification flaws produced in the current study in Figure 10 follow the typical range and average values of the "ENIQ" flaws. In the graphs the range and average values for the weld joined fatigue surfaces show roughly 50% smaller values than for the solidification flaws, but still exhibit bigger values than most of the service-induced flaws. The opening range of thermal fatigue cracks produced in this study is in the area of most of the service-induced cracks. There is no average value given for the thermal fatigue cracks because the openings can be manipulated to specified value.

Figure 11 shows that the range and average values of the crack tip opening for the "ENIQ" flaws lay markedly in bigger values than for the service-induced cracks. However, for the flaws produced in current study the crack tip values for the solidification cracks show only a bit higher values than for the service-induced flaws. For the weld joined fatigue surfaces and thermal fatigue cracks the values are clearly smaller than those reported for the service-induced cracks. This difference can be attributed to the different measurement processes used by different authors, as described in the caption text of Figure 11.

The effect of flaw characteristic on the reliability of sizing

The crack characteristics may influence sizing reliability by affecting the likelihood of correct identification of crack tip signal. The stronger the tip signal is, the easier it is to correctly distinguish it from microstructural noise. The crack opening, and crack tip opening in particular, may affect the strength of the crack signal. Secondly, the artificial flaws may have "false tip candidates", i.e. features other than the deepest tip that give tip-like signal and thus may easily be misinterpreted as the crack tip. For example, strong twists or branches with secondary tips may act this way.

As shown in Figures 6-9, weld joined fatigue surfaces and solidification cracks may show features that can act as "false tips". In contrast, thermal fatigue flaws do not exhibit such false tips. The effect of these features to ultrasonic inspection performed is analyzed in more detail in [10].

The used flaw manufacturing techniques caused characteristic opening profiles both in the surface and depth direction. As a result of the nature of the manufacturing process, the solidification flaws have the greatest opening values of all the flaws. Opening of solidification flaws cannot be manipulated and it is result of the solidification process. Also for weld joined fatigue surfaces, there is limited possibility to control the resulting flaw opening values.

The production process for thermal fatigue cracks allows control of the opening profile both in the surface and depth direction. This capability was demonstrated in this study.

One aim of the work was to reveal the effect of different openings of the manipulated thermal fatigue cracks to obtained NDE response. However, as detailed in the other publication [10], other features present in the samples proved to dominate the ultrasonic response and no distinct effect of the crack opening could be observed.

In order to ensure relevance of training and reliability of qualification, the selection of flaws used should be based on good knowledge of flaw characteristics. Any potential "false tips" etc., which may lead to misinterpretation, should be noted and accounted for. Sizing based on "false tip" does not correspond to actual in service inspection. In particular, if there are false tips near the true tip (such as the examples show in Figures 6 and 8) erroneous interpretation based on the false tip may give sizing result close to the true crack size. In such a case, apparently accurate sizing of the flaw with false tip does not indicate accurate sizing in actual in-service inspection. Consequently, flaws with false tips may not be used reliably in qualification or performance demonstration, as they may give overly optimistic impression of the inspection performance.

Future studies

The results of this work revealed clear needs for future studies. Such studies should include the effect of weld noise to tip signal detection from thermal fatigue cracks, and crack detection reliability of different inspection techniques.

CONCLUSIONS

The following conclusions can be drawn from the study:

1) Thermal fatigue cracks can be produced, with the stated tolerances, without causing any additional disturbances. This was shown both by the metallographic images and NDE results.
2) All the flaw types included in this study produce tip signal that can be identified by at least some of the ultrasonic techniques used. None of the cracks were so tight as to become completely transparent to ultrasound.
3) The weld joined fatigue surfaces may have twists that give signal that was erroneously interpreted as the crack tip. This feature of the flaw type results in tendency to undersize the crack and decreased average error (when compared to cases when such "false tip" was not available and inspectors have instead interpreted microstructural noise as the crack tip).
4) The solidification crack may have branching and multiple crack tips. This feature of the flaw type results in tendency to undersize the crack and decreased average error (when compared to cases when such "alternate tip" was not available and inspectors have instead interpreted microstructural noise as the crack tip).
5) Thermal fatigue flaws showed no "false tips" to be identified. Consequently, mechanized and phased array ultrasonic inspections could locate the correct crack tip in the simple geometry, and low noise base material sample. In contrast, the manual inspections often failed to correctly identify the crack tip even in this simple case, but analysed signals from random microstructural noise.
6) The effect of the weld material was seen for the solidification flaws and weld joined fatigue surfaces. In this study the thermal fatigue cracks were located in the low noise base material, but if they had been in the weld material, it may be speculated that the mechanised and phased array techniques would have had difficulties in detecting signal from the crack tip.
7) Furthermore, opening manipulation of thermal fatigue cracks showed marked effect on the opening profiles as seen both in metallographic images and some NDE results.
8) The flaws included in this study give a representative sample of artificial flaw production techniques and artificial flaws in use today.
9) The performance of the manual inspection techniques is poorer than was expected, especially considering the simple, low noise, component in question.
10) The "false tip" features that may be present in solidification cracks and weld joined fatigue surfaces may lead to misleading results if used in qualification or performance demonstration.
11) Future studies could include studying the effect of weld noise to thermal fatigue crack tip signal detection and overall detection capability of different techniques.

REFERENCES

1) Wüstenberg, H. and Erhard, A., "Problems with Artificial Test Reflectors at the Performance Demonstration of Ultrasonic Inspections" 6th European Conference *on Non Destructive Testing*, Nice, pp. 741-746, 1994
2) ENIQ, "Final Report of the First ENIQ Pilot Study", ENIQ Report nr 20, EUR 19026 EN, European Commission, JRC Petten, 38 p., 1999.
3) Iacono I, Eriksen B, Mendes J, Metten L, Lofaj F, Seldis T and Wallendorf M, *NESC III Inspection Task Group, Destructive Examination Report, RRT Dissimilar Metal Weld Component*, EC DG JRC Institute for Energy. EUR 22607 EN ISSN 1018-5593, 2006.
4) Kemppainen, M., *Realistic artificial flaws for NDE qualification – novel manufacturing method based on thermal fatigue*. Dissertation for the degree of Doctor of Science in Technology. Espoo, Finland, 2006. (Available online from: http://lib.tkk.fi/Diss/2006/isbn9512282631/)

5) Becker, F.L., Doctor, S.R., Heasler, P.G., Morris, C.J., Pitman, S.G., Selby, G.P. and Simonen, F.A., "Integration of NDE Reliability and Fracture Mechanics - Phase I Report", *NUREG/CR-1696 PNL-3469,* Vol 1, 170 p., 1981.

6) Yoneyama, H., Senoo, M., Miharada, H. and Uesugi, N., "Comparison of Echo Heights between Fatigue Crack and EDM Notch", 2nd International Conference *on NDE in Relation to Structural Integrity for Nuclear and Pressurized Components*, New Orleans, Louisiana, U.S.A., 8 p., 2000

7) Kemppainen, M., Virkkunen, I., Pitkänen, J., Hukkanen, K. and Hänninen, H., "Production of Realistic Flaw in Inconel 600", Conference *on Vessel Penetration 13 Inspection, Crack Growth and Repair*, USNRC and Argonne National Laboratory, Washington D.C., Gaithersburg, USA. *NUREG/CP-0191*, Vol. 1, pp. 51-60 and Vol. 2, pp. 181-196 (presentation slides), 2003.

8) Wåle, J. & Ekström, P., *Crack Characterisation for In-Service Inspection Planning*. SKI-project 14.4-940389, SAQ/FoU report 95/07, SAQ Kontroll Ab, Stockholm, Swerige, 1995.

9) Lemaitre, P., Iacono, I. & Vergucht, P. (eds.), *Results of the Destructive Examination of the ENIQ Pilot Study: Defect Catalogue*, ENIQ Report 19, EUR 19024 EN, JRC Petten, The Netherlands, 1999.

10) Packalen, T, Sillanpää J, Kemppainen M, Virkkunen I, Paussu R, "The influence of the crack opening in the UT inspection qualification", 6th International Conference *on NDE in Relation to Structural Integrity for Nuclear and Pressurized Components*, Budapest, Hungary, 2007. *To be published.*

11) Virkkunen, I., Kemppainen, M. and Pitkänen, J., "Effect of Crack Opening on UT Response" *The e-Journal of Nondestructive Testing & Ultrasonics*, ISSN: 1435-4934. 11(11), Nov 2006. 9 p.
(Available online from: http://www.ndt.net/article/ecndt2006/doc/Th.4.4.2.pdf)

12) Paussu R, Virkkunen I, Kemppainen M, "Utility aspect of applicability of different flaw types for qualification test pieces", 6th International Conference *on NDE in Relation to Structural Integrity for Nuclear and Pressurized Components*, Budapest, Hungary, 2007. *To be published.*

Annex 1 Results for measured flaw characteristics; specified target size, best estimate values for the thermal fatigue cracks (as given by the manufacturer), and true values as the results of the destructive testing.

Flaw ID	Target		Produced best estimate			True					
	Length (mm)	Depth (mm)	Surface opening (µm)	Length (mm)	Depth (mm)	Surface opening (µm)	Depth (mm)	Mouth (µm)	Middle (µm)	Tip region (µm)	Tip radius (µm)
186AGB364	6	3	80	7,7	-	80	4	96	73	33	1,5
193AGB367	6	3	160	11,2	-	100	4,3	88	66	50	2,2
211AGB385	6	3	40	6,9	3,2	60	3,2	101	30	20	0,4
218AGB389	6	3	120	8,1	3,2	80	3,3	54	44	12	0,4
235AGB395	12	6	120	21,7	6,5	140	6,2	104	54	20	0,8
237AGB396	12	6	40	20	6,5	75	5,8	67	40	14	0,1
239AGB398	12	6	160	20,9	6,5	150	6,5	95	60	43	5,5
250AGB405	12	6	80	19,4	6,5	105	5,7	101	62	23	4,8
139AHF101		3	-	-	6,5 *	-	5,7	68	53	21	3,9
139AHF102		6	-	-	9,7 *	-	8,1	149	102	12	0,5
139AHF103		3	-	-	6,9 *	-	5,4	133	68	53	0,3
139AHF104		6	-	-	10,0 *	-	7,8	105	92	64	0,7
139AHP101		10	-	-	10,0	-	9,2	86	129	130	3,6
139AHP102		6	-	-	6,5	-	6,5	126	110	31	10,2
139AHS101		3	-	-	8,2 *	-	6,9	191	233	44	9,1
139AHS102		3	-	-	7,7 *	-	6,4	227	149	38	12,5
139AHS103		6	-	-	9,4 *	-	8	184	255	87	14,9
139AHS104		6	-	-	10,0 *	-	9	158	217	151	5,7

* Depth values are before machining of root surface of the weld joint. Machining thickness is unknown.